An experiment on second-order capillary gravity resonant wave interactions

By L. F. McGOLDRICK

Department of the Geophysical Sciences, The University of Chicago

This paper presents the results of a set of detailed experimental measurements on the resonant interaction of capillary-gravity waves for a case in which the entire propagation is in one direction. The influence of viscous attenuation is accounted for in the analysis. The measurements trace the entire spatial variation, or modulation envelope, of the amplitudes of the interacting modes from their inception near a wave-maker to their ultimate extinction through viscous dissipation, in excellent agreement with the theory. This is an unambiguous demonstration that at resonance and for the initial conditions specified at the wave-maker, a wave of uniform profile cannot exist.

1. Introduction

In recent years there has been an intense interest in the non-linear theory of wave propagation in dispersive systems. Just several years ago a discussion meeting was organized by M. J. Lighthill† concerning the remarkable progress made in this difficult field in the six or so years prior to that meeting. It would be presumptuous to review all of that progress here. However, it will be illuminating to present a brief background against which the investigations to be reported in this paper may be compared.

Stokes (1847) was the first to consider the effects of non-linearity on periodic progressive gravity waves of permanent form on water of infinite depth. On the *assumption* that a finite amplitude wave of uniform profile (temporally and spatially) existed, he produced by a perturbation expansion an approximate expression for the form and speed of such a wave. In the field of water waves, at least, this now familiar method of approximation traditionally bears his name. Stokes, Rayleigh (1917) and others have carried the approximation to the fifth order in an expansion parameter ϵ, say, which is proportional to the maximum slope of the waves and is assumed small. Benjamin & Feir (1967), however, have established analytically and experimentally the remarkable result that Stokes waves, while representing theoretically possible states of dynamic equilibrium *are in fact unstable*, the instability arising from what amount to third-order terms in the Stokes expansion. It is of course essential to their work that the assumption of a completely uniform state be discarded.

† The proceedings of that meeting appear in *Proc. Roy. Soc. Lond.* A **299**, 1456 (1967).

The theory of the non-linear interaction of several intersecting trains of gravity waves was first presented by Phillips (1960). He showed by a Stokesian type perturbation analysis that for certain quartets of progressive gravity waves, a secularity among the third-order terms in the analysis will arise. He interpreted this as indicating that the amplitude of one of the members of this resonant quartet will grow linearly with time as it progresses, at least until the conditions imposed by the perturbation analysis are no longer applicable. This implies the absence of a uniform state for wave combinations satisfying the now well-known selective resonance conditions.

Benney (1962) re-investigated the theory of resonant interactions by abandoning *ab initio* the assumption of a uniform state for resonant quartets. Under the assumption that the amplitudes of all the waves participating in the resonance are slowly varying functions of time, he obtained in principle solutions valid for longer time than were those of Phillips.

The theory of these resonant interactions aroused something of a mild controversy, which was not resolved until Longuet-Higgins & Smith (1966) and independently McGoldrick, Phillips, Huang & Hodgson (1966) presented detailed experimental measurements confirming the main predictions of the theory. It was Longuet-Higgins (1962), who first saw the need for these experiments and suggested a suitable experimental configuration. Both groups of investigators, however, were severely limited by the size of the experimental facilities. Because of the weakness of these gravity wave interactions, only the initial linear growth of one of the interacting components was observed. For completeness and other reasons, which seemed compelling at that time, the *selectivity* of the interactions was investigated with considerably more attention. Both sets of experiments have been summarized and compared by Phillips (1967), who shows in the same work the intimate relationship between these resonant interactions and the Benjamin–Feir instability mentioned above.

For waves of sufficiently short length that the effects of capillarity become important, the attack on the influence of non-linearity has followed much the same road. Harrison (1909) computed a Stokes type approximation for a single train of capillary-gravity waves to the third order. He noticed that for wave-numbers less than a certain critical wave-number $k^* = (g/2\gamma)^{\frac{1}{2}}$ (g is the acceleration due to gravity, γ is the ratio of the surface tension coefficient to the density of the fluid), the influence of the non-linearities is to distort the wave profile in such a way that the crests are sharpened and the troughs flattened. This is consistent with the well known approximately trochoidal form found by Stokes for the longer gravity waves, and profiles of this type are called gravity-type profiles. For wave-numbers larger than k^*, the distortion is in the opposite sense. The so-called capillary-type profiles are flattened at the crests and sharpened at the troughs. We now know that this is consistent with the *exact* profiles calculated by Crapper (1957) for pure capillary waves. Harrison noted in passing that the approximation breaks down when the wave-number is exactly k^*. For this wave-number, the Stokesian analysis predicts a second harmonic distortion of the basic sinusoidal profile that has infinite amplitude, clearly violating the conditions of the perturbation procedure.

Wilton (1915), apparently unaware of Harrison's work, carried the perturbation procedure to the fifth order, finding the same singularity present at all orders of approximation, occurring at wave-numbers $k = (g/n\gamma)^{\frac{1}{2}}$, $n = 2, ..., 5$. He then attempted to remove this singularity for the second-order analysis ($n = 2$) by including in the basic (unperturbed) state a second harmonic constituent of arbitrary (but constant) amplitude, which was to be determined in such a way as to effect the disappearance of the singularity. He retained, however, the assumption that a steady state existed.

A little known paper, Kamesvara Rav (1920) investigated the forms of finite amplitude capillary-gravity waves on water of finite depth by a Stokesian analysis to the third order of approximation with the inevitable appearance of the same singularity at the second order, but in this case somewhat disguised by the formidable algebraic combinations of hyperbolic functions usually attendant with problems involving finite depth. More important, he showed photographs of experimentally produced waves near the singular configuration clearly indicating pronounced second harmonic distortion, which he called 'doubling of the crests.' Unfortunately, he did not present detailed experimental results.

Pierson & Fife (1961) reproduced Wilton's results for capillary-gravity waves, including both the singular case and the cases for which the perturbation analysis is valid. They then investigated the situation in the immediate neighbourhood of the singularity by the method of strained co-ordinates. Again, their work postulates the existence of a uniform state.

If the assumption of a uniform profile is abandoned *ab inito*, then it is possible to investigate these singular cases in the frame-work of resonant interaction theory. McGoldrick (1965) presented a detailed theoretical investigation of resonant interactions among these capillary-gravity waves and among pure capillary waves. But, unlike the gravity wave resonances, the interaction occurs at the second order, and is somewhat less tedious to analyze. In particular, McGoldrick obtained an energy integral for the interacting waves and completed the solution for the time-varying amplitudes in terms of elliptic functions. Relevant to the remainder of this present paper, he showed that the second-order singularity of Wilton and of Pierson & Fife may be eliminated by interpreting the phenomenon as a particular case of these resonant interactions. Unfortunately, McGoldrick's solution for this configuration is incorrect due to some algebraic errors, and will be corrected here.

None the less, despite the growing body of theoretical literature in this field, and contrary to the direct experimental evidence produced by Longuet-Higgins & Smith (1966) and by McGoldrick *et al.* (1966), uniform profile solutions have still recently been proposed for resonant conditions. Sullivan (1966) has produced such solutions for intersecting capillary-gravity waves by the method used by Pierson & Fife corresponding to the resonant conditions presented by McGoldrick (1965). Barakat & Houston (1968), evidently unaware of the work of Kamesvara Rav, have trod much the same ground, and have sorted out the algebra to identify the same second-order singularity in the case of finite depth, which they go on to eliminate by Wilton's method.

It appears that it is necessary, once again, to demonstrate that resonant con-

ditions preclude the *physical* existence of a uniform wave profile solution for certain initial conditions. Accordingly, an experiment has been undertaken, and the results, as will be seen, are clearly and conclusively contrary to the uniform profile assumption and confirm in detail the resonant solution presented here.

Section 2 will be devoted to a brief review of the theory of the interaction, with a reduction of the solutions to the case most easily observable in the wave tank, which will be called 'second harmonic resonance' (and to which, for comparison, the results of Wilton and of Pierson & Fife supposedly correspond). In §3, the modifications of the interaction due to the inevitable attenuating influence of molecular viscosity will be introduced, since the proper interpretation of the experimental results is heavily dependent on a critical assessment of the dissipative process involved.

Following a brief description of the experimental apparatus with some pertinent comments on technique, the results of several series of experiments will be presented in §5. In particular, the amplitudes of each of the interacting components will be traced from their inception close to an oscillating wavemaker through their ultimate viscous decay with increasing distance from the source.

Before turning to §2, it should be pointed out that much of the analysis presented here has been performed by Simmons (1967) in a generalization of McGoldrick's earlier work. By allowing the amplitudes *and* phases of the interacting waves to be slowly varying functions of both space and time, Simmons has shown that the resonant response in general involves both amplitude and phase modulations simultaneously. It is only with special initial conditions that the phase modulations disappear, namely that the relative phase at some time be exactly $\frac{1}{2}\pi$. If this is assumed *ab initio*, as was done by the earlier investigators, then the response is one of amplitude modulation alone. On the other hand, if the relative phase is zero, the amplitude modulations disappear altogether, and the system responds with a slow linear modulation of the phases, which amounts to an $O(\epsilon)$ frequency (or wave-number) shift. That these latter so-called 'steady state', or permanent form, solutions are contained within the framework of resonance theory is a remarkable result of Simmons's generalization.

Clearly then, the initial conditions are critical in determining the resonant response. For the remainder of this paper, it should be kept clearly in mind that the initial conditions for the experimental investigation have been chosen to elicit a response consisting solely of amplitude modulations.

2. Review of the theory

For resonant interactions to occur at the second order, it is sufficient to consider the mutual interactions of a triad of surface waves. Accordingly, we represent the free surface displacement as the sum of three waves satisfying the resonance conditions. That is, let

$$\zeta(\mathbf{x}, t) = \sum_{i=1}^{3} a_i(\mathbf{x}, t) \cos \psi_i, \tag{2.1}$$

where the phase function is

$$\psi_i = \mathbf{k}_i . \mathbf{x} - \omega_i t - \eta_i$$

and the wave-numbers and frequencies are such that

$$\left. \begin{array}{l} \mathbf{k}_1 + \mathbf{k}_2 + \mathbf{k}_3 = \omega_1 + \omega_2 + \omega_3 = 0 \\[2mm] \omega_i^2 = g k_i + \gamma k_i^3 \quad (i = 1, 2, 3). \end{array} \right\} \tag{2.2}$$

and

The wave-numbers and frequencies are constant here, and for the purposes of this paper, the arbitrary phase angles η_i will be supposed constant. The amplitudes a_i are considered to be slowly varying functions of both space and time in the sense that the fractional changes of amplitude are small over a typical wave-length and wave-period. Numerical solutions of the resonance conditions (2.2) were given by McGoldrick (1965), and Simmons (1967) has shown a clever geometrical construction for the resonant triads.

The dynamical equations governing the amplitudes of the interacting components were first obtained by McGoldrick (1965) by a straightforward perturbation procedure. We shall use the more concise development of Simmons who showed by variational methods that, correct to the second order, the three dynamical equations for the amplitudes of the interacting components can be expressed compactly as

$$\frac{1}{2} \left\{ \frac{\partial}{\partial t} a_i^2 + \mathbf{U}_i . \nabla a_i^2 \right\} = a_1 a_2 a_3 J / c_i \quad (i = 1, 2, 3). \tag{2.3}$$

In these equations, $c_i = \omega_i / k_i$ is the phase speed and $\mathbf{U}_i = \nabla_{\mathbf{k}} \omega_i$ is the group speed of the ith interacting component, and the interaction coefficient J is given by

$$4J = - \sum_{j=1}^{3} \omega_j \omega_{j+1} (1 + \mathbf{1}_j . \mathbf{1}_{j+1}), \tag{2.4}$$

where the subscripts j are to be interpreted modulo 3, and $\mathbf{1}_j = \mathbf{k}_j / k_j$ is a unit vector in the direction of propagation of the jth component. J, c_i and $\mathbf{U}_i$ are of course constants for any given configuration satisfying (2.2). Further, the constant phase angles η_i satisfy

$$\eta = \sum_{i=1}^{3} \eta_i = \tfrac{1}{2}\pi, \tag{2.5}$$

where η may be called the total phase.

The mean wave energy E_i and momentum $\mathbf{M}_i$ per unit projected surface area for each mode can be written as $E_i = \tfrac{1}{2}\rho \omega_i c_i a_i^2$ and $\mathbf{M}_i = \tfrac{1}{2}\rho \mathbf{k}_i c_i a_i^2$. Since there is no dissipation and no net horizontal forces are acting, energy and momentum integrals exist for the dynamical system (2.3). We easily see that two independent integrals,

$$\left. \begin{array}{l} \sum_{i=1}^{3} \dot{E}_i + \mathbf{U}_i . \nabla E_i = \rho a_1 a_2 a_3 J \sum_{i=1}^{3} \omega_i = 0 \\[4mm] \sum_{i=1}^{3} \dot{\mathbf{M}}_i + (\mathbf{U}_i . \nabla) \mathbf{M}_i = \rho a_1 a_2 a_3 J \sum_{i=1}^{3} \mathbf{k}_i = 0, \end{array} \right\} \tag{2.6}$$

and

exist by virtue of (2.3) and the kinematic resonance conditions (2.2). In the absence of viscosity, then, the total energy density and momentum density are

conserved. The principal dynamical effect of these interactions, then is to continuously redistribute these quantities among the interacting components.

The interaction equations obtained by McGoldrick are a special case of Simmons' equations (2.3) for which the amplitudes of the interacting waves are only functions of time. It is clear from the form of (2.3) that for the cases in which the resulting amplitude modulations appear to be steady, but spatially varying, it is only necessary to replace $\partial/\partial t$ in the earlier equations by $(U_i . \nabla)$. The solutions for the modulation envelopes in all cases have been completed in terms of Jacobian elliptic functions and have been investigated in some detail.

If the three wave-numbers are co-linear so that the propagation is in one direction, then it is still possible to satisfy the resonance conditions. In particular, if two of the wave-numbers coincide, say $\mathbf{k}_1 = \mathbf{k}_3$, then the resonance conditions require that $\mathbf{k}_1 = \mathbf{k}_3 = -\frac{1}{2}\mathbf{k}_2$ and $\omega_1 = \omega_3 = -\frac{1}{2}\omega_2$. That is, both the wave-number and frequency of the mode completing the triad are double that of the other mode. This degenerate case involves only two identifiable modes instead of the usual three, and is easily interpreted as being a dynamical resonance between a fundamental $(\mathbf{k}_1, \omega_1)$ and its own second harmonic $(\mathbf{k}_2, \omega_2)$ both propagating in the same direction with identical phase speeds. In virtue of the dispersion relation given in (2.2), we can easily see that if we denote by $c_m = (4g\gamma)^{\frac{1}{4}}$ the minimum value of the phase speed for capillary-gravity waves, then the phase speed $c_1 = c_2 = (9/8)^{\frac{1}{4}}c_m$, and the wave-number and frequency of the fundamental mode are $k_1 = (g/2\gamma)^{\frac{1}{2}} = k^*$ and $\omega_1 = (9g^3/8\gamma)^{\frac{1}{4}}$. For clean water at room temperature, the fundamental has a wavelength of about 2·4 cm and frequency about 9·8 c/s, travelling with its second harmonic at a speed 3 % greater than the minimum value of 23·2 cm/s.

For this case of second harmonic resonance, two of the dynamical equations ($i = 1$ and $i = 3$) in (2.3) are identical since there are really only two modes present. Further, since in this situation $M_i = E_i/c_1$, the integrals (2.6) are no longer independent, being in fact identical to within a constant multiplier (the phase speed). Since the 1 and 3 modes are indistinguishable, we are at liberty to assume without loss of generality that the amplitudes a_1 and a_3 and the phases η_1 and η_3 are identical and write a linear combination of these two modes as

$$\zeta_1(x, t) = \hat{a}_1(x, t) \cos{(k_1 x - \omega_1 t)}, \tag{2.7}$$

where $\hat{a}_1 = (a_1 + a_3)/\alpha$ and the phase has been chosen to be zero. The constant α will be determined below. The remaining mode (the second harmonic) is now

$$\zeta_2(x, t) = a_2(x, t) \cos{(2k_1 x - 2\omega_1 t - \tfrac{1}{2}\pi)}$$

using the condition that the total phase is $\frac{1}{2}\pi$. The dynamical equations are obtained simply by adding the first and third of equations (2.3) and retaining the second as it is, or

$$\frac{1}{2}\left(\frac{\partial}{\partial t} + U_1 \frac{\partial}{\partial x}\right) \hat{a}_1^2 = -\frac{\omega_1 k_1}{2} \hat{a}_1^2 a_2,$$

$$\frac{1}{2}\left(\frac{\partial}{\partial t} + U_2 \frac{\partial}{\partial x}\right) a_2^2 = +\frac{\alpha^2 \omega_1 k_1}{8} \hat{a}_1^2 a_2, \tag{2.8}$$

where use has been made of the fact $a_1 a_3 = \frac{1}{4}\alpha^2 \hat{a}_1^2$ and the interaction coefficients have been determined from (2.4) for this configuration.

The constant α is now determined by noting that the modified equations (2.8) for this degenerate case must still satisfy the energy integral (2.6) and straight-forward substitution reveals easily that $\alpha = \sqrt{2}$. Simmons obtained these same interaction equations for second harmonic resonance by starting the analysis *ab initio* with only the two modes present. The short-cut used here is clearly equivalent to his method.

For the remainder of this paper, we shall assume that the amplitudes $\hat{a}_1$ and a_2 are independent of time. This, as will be seen in §5, corresponds to the experimental arrangement used where the waves are created by an oscillating wavemaker. The amplitude modulation pattern appears steady then, but the modulation envelope varies spatially in the direction normal to the plane wave-maker.

Omitting now the circumflex on the fundamental amplitude, then we have

$$\left.\begin{aligned}\frac{da_1}{dx} &= -\frac{\omega_1 k_1}{2U_1} a_1 a_2, \\ \frac{da_2}{dx} &= +\frac{\omega_1 k_1}{4U_2} a_1^2.\end{aligned}\right\} \tag{2.9}$$

Choosing as initial conditions $a_1(x_0) = a$, $a_2(x_0) = 0$, then the solution of (2.9) is

$$\left.\begin{aligned}a_1(x) &= a \operatorname{sech}\left[\frac{a\omega_1 k_1}{\sqrt{(8U_1 U_2)}}(x - x_0)\right], \\ a_2(x) &= a\left(\frac{U_1}{2U_2}\right)^{\frac{1}{2}} \tanh\left[\frac{a\omega_1 k_1}{\sqrt{(8U_1 U_2)}}(x - x_0)\right].\end{aligned}\right\} \tag{2.10}$$

We can define an interaction length scale L for later reference as being the distance over which the fundamental a_1 decays to $1/e$ of its maximum attainable value a. Then

$$a k_1 L \doteq 1 \cdot 66(8U_1 U_2)^{\frac{1}{2}}/\omega_1,$$

or since

$$U_1 = \tfrac{5}{6}c_1 \quad \text{and} \quad U_2 = \tfrac{7}{6}c_1,$$

we have

$$L \doteq 1 \cdot 8(ak_1)^{-1}\,\text{cm}. \tag{2.11}$$

for clean water at room temperature. The interaction length is inversely proportional to the maximum slope attained by the fundamental wave. In other terms, since the total energy flux is constant *via* integration of (2.6), the interaction length is proportional to the $(-\frac{1}{2})$ power of the total energy flux.

Figure 1 is a sketch of those salient features of this interaction which should be observable in a small wave-tank. The amplitudes a_1 and a_2 are shown as a function of distance. Note that the wave profiles are changing shape as they progress and that they are not symmetrical about a vertical line drawn through the crest of the fundamental. This is to be contrasted with the symmetrical profiles of Wilton and of Pierson & Fife for which the amplitudes are spatially uniform.

A natural set of initial conditions for experimentation becomes clear upon examination of figure 1. A wave closely approximating the fundamental alone can be created very close to a wave-maker oscillating at frequency ω_1, corresponding to the position indicated by the ordinate in this figure. Within the distance of several interaction lengths L this fundamental should be virtually undetectable, having transferred nearly all its energy into its own second harmonic, at frequency $2\omega_1$ which arises $\frac{1}{2}\pi$ out of phase with the fundamental.
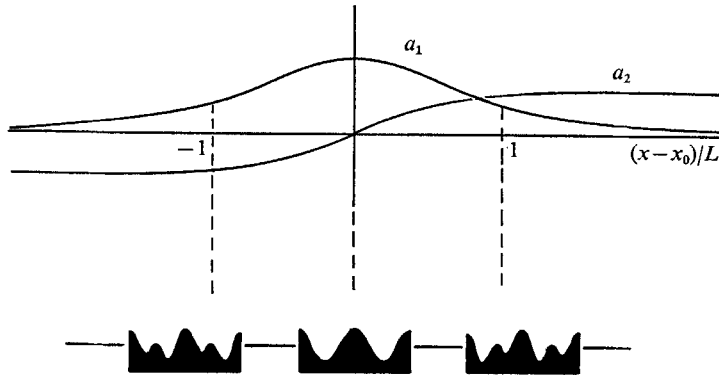
FIGURE 1. Amplitudes of the interacting modes as a function of distance according to (2.10). L is the interaction length (2.11). The sketches below show the (vertically exaggerated) wave-form, which is asymmetrical except at $x = x_0$.

As a consequence of this interaction, we are led to the following remarkable fact: a purely sinusoidal wave of wave-number $(g/2\gamma)^{\frac{1}{2}}$ of any amplitude cannot propagate indefinitely on an inviscid liquid, and can exist only as a transient state. In other words, for this wave-number, *the solution to the linear problem represents a theoretically possible state of dynamical equilibrium to the lowest order which is in fact unstable at the next order of approximation.* This is precisely what Benjamin & Feir found for the second-order Stokes wave, which they showed to be unstable at the next order. The difference, of course, is that for our case here, dynamically significant resonances occur at a lower order than is possible for gravity waves.

3. The influence of viscous dissipation

Before proceeding with the experiment suggested by figure 1, it is prudent to examine the approximate effects of viscosity on the dynamics of this interaction. It is well known† that the influence of viscous dissipation is to attenuate the waves exponentially with distance from the generating source, the modulus of decay (logarithmic decrement) being given by $\Delta = 2\nu k^2/U$ per unit distance, *provided* the surface be scrupulously clean and the wave-Reynolds number $R_w = \omega/\nu k^2$ be large. If the decay length Δ^{-1} of the most rapidly attenuated

† See, Lamb (1932, § 348).

wave is much greater than the interaction length L, then the interaction will proceed relatively unimpeded by viscosity. This requires, then, that $L\Delta \ll 1$. For the case of second harmonic resonance it is a simple matter to show that this requirement is $ak_1 \gg 32R_w^{-1}$ approximately, for clean water.

Under these circumstances considering the effects of viscosity to be only a small perturbation to the interaction, it is appropriate to include these decay terms in the dynamical equations (2.9) as follows:

$$\left. \begin{aligned} \frac{da_1}{dx} &= -\frac{\omega_1 k_1}{2U_1} a_1 a_2 - \Delta_1 a_1, \\ \frac{da_2}{dx} &= +\frac{\omega_1 k_1}{4U_2} a_1^2 - \Delta_2 a_2. \end{aligned} \right\} \tag{3.1}$$

Here, Δ_1 and Δ_2 are the logarithmic decrements obtained for the fundamental and the second harmonic from the linear theory, which for clean water are $\Delta_i = 2\nu k_i^2/U_i$. The results will indicate that (3.1) seems adequate at least for the parameter values obtaining in this experiment.

Analytical solutions of the weakly damped non-linear system represented by (3.1) cannot be written in closed form with the exception of a few isolated (and physically irrelevant) cases. Approximate solutions, valid only for propagation distances of the order of an interaction length L, have been obtained by McGoldrick (1965), but they are too cumbersome for practical use. It is a very simple task, however, to obtain solutions by analogue computation (or numerical integration). Since the system is autonomous, all of the relevant details of the solution can be presented most compactly by determining the families of trajectories in the (a_1, a_2) phase plane as a function of the initial conditions $(a_1(x_0), a_2(x_0))$ and (parametrically) the logarithmic decrements Δ_1 and Δ_2.

Figure 2 is a family of trajectories for the case of clean water at room temperature. The amplitude of the second harmonic, a_2, is plotted on the ordinate and that of the fundamental on the abscissa, and the trajectories are travelled in the counterclockwise sense. That is, distance measured away from the source is increasing along each trajectory in the sense toward the origin.

Each trajectory crosses the abscissa only once with the sole exception of that trajectory coinciding with the ordinate. For a given trajectory (that is, given the initial conditions at the source), the maximum possible fundamental occurs when the trajectory has a vertical tangent. The locus of these points is given by $a_2 = -2\Delta_1 U_1/\omega_1 k_1$ ($=$ constant) which is shown as the dashed horizontal line in the lower quadrant. The maximum positive value of the second harmonic occurs where the trajectories have horizontal tangents; the locus is the dashed parabola $a_2 = a_1^2 \omega_1 k_1/4U_2\Delta_2$ indicated in the first quadrant. Finally, in the inviscid limit $\Delta_1 = \Delta_2 = 0$, these loci coincide with the abscissa and the ordinate respectively, and the trajectories become the ellipses $U_1 a_1^2 + 2U_2' a_2^2 =$ constant, corresponding to the inviscid solution (2.10).

Consider the initial conditions corresponding to those suggested near the end of the preceding section, viz. any point on the abscissa. Clearly, a purely
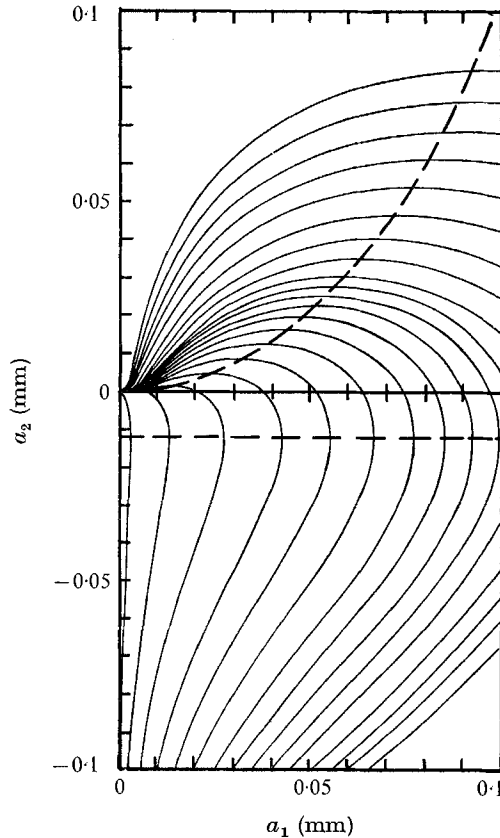
FIGURE 2. Phase plane trajectories for the case of clean water at room temperature. Below the dashed parabola the energy transfer is primarily due to interaction, and above the viscous effects dominate.

sinusoidal wave of wave-number $(g/2\gamma)^{\frac{1}{2}}$ cannot decay because of viscous dissipation without first creating its own second harmonic, $\frac{1}{2}\pi$ out of phase, which will grow through resonant interaction until the resonant growth rate is balanced exactly by the viscous decay rate, from which point both will decay and ultimately be extinguished. This in fact is clear from the second equation of (3.1). And this is precisely what will be shown by the experiment.

4. The equipment and technique

The tank in which the experiments were performed is rectangular, with length about 3 m and width about 61 cm, filled with ordinary tap water to a depth of 44 cm, effectively placing the waves in infinitely deep water. The construction is of plywood with plexiglass sides supported within a rigid slotted steel angle framework.

Waves are created by oscillating vertically a triangular shaped plunger extending the width of the tank. The height of the plunger is about 5 cm and

the front face is covered with a smooth thin sheet of glass, inclined forward at an angle of about 20° with the vertical. Because of the smoothness and cleanliness of the glass face, the progressive waves produced are remarkably straight crested and of quite uniform amplitude along the direction of the crests.

The plunger is mounted on a rigid vertical shaft confined to a fixed axis with ball bushings (linear motion bearings) and is fastened concentrically to the 7·5 cm diameter voice coil of a heavy permanent magnet from a loudspeaker (Jensen, Model G 610). The entire wave-maker unit is mounted in rigid structure physically separate from the wave tank itself eliminating unwanted vibrations and spurious waves. The plunger is driven by a suitable electronic signal delivered to the voice coil (16 ohms) by a transistorized 40 W power amplifier. The frequency response of the amplifier is flat to within $\frac{1}{4}$ db from d.c. to 10 KHz.

The primary driving source used in this experiment is a laboratory sine wave generator. The instantaneous vertical position of the plunger is determined from a linear displacement voltage transducer, the output of which is a voltage directly proportional to the position. This voltage is compared with the primary driving signal, and the difference (error signal) is fed back through the power amplifier continuously in such a way that the error is reduced (effectively) to zero. This feedback system assures that the actual motion of the plunger is a faithful reproduction of the desired driving signal. The advantages of this driving system over the usual motor and eccentric crank system are obvious: no spurious harmonics of the fundamental frequency are introduced due to mechanical linkages, and the frequency and amplitude of the plunger motion (whence that of the created waves) are continuously and independently adjustable. The amplitude and frequency stability of the motion is that of the oscillator itself, typically one part in 10^5.

Measurements of the instantaneous wave profile at any point in the tank are made with a wave probe similar to the well-known capacitance type. The probe element itself, however, is *not* a pure coaxial capacitor, but a no. 30 bare stainless steel hypodermic needle; the total electrical impedence with respect to a fixed ground is inversely proportional to the depth of immersion. Driven from a high-frequency constant voltage oscillator, the current through the probe is directly proportional to the immersion depth, and suitable detection by simple transistor circuits produces a voltage signal directly proportional to the instantaneous wave height. Overall sensitivity of the device is 1·414 V/mm wave height, with a frequency response flat from d.c. to at least 100 c/s, and is remarkably linear. With proper attention, wave amplitudes of the order of 10^{-3} mm can easily be detected.

We wish to create in the immediate vicinity of the plunger a purely sinusoidal wave of wave-number k_1. This can be accomplished with some precision by oscillating the plunger sinusoidally at the corresponding frequency, given by the dispersion relation in (2.2). Since for second harmonic resonance $k_1 = (g/2\gamma)^{\frac{1}{2}}$ and $\omega_1 = (9g^3/8\gamma)^{\frac{1}{4}}$, these values depend solely on the value of the surface tension coefficient γ. It is a simple matter to measure the static value of γ with a duNouy tensiometer. Further, it was always a pleasant coincidence that the measured values of γ for our tap water agreed with the accepted static

values determined for distilled water,† the agreement usually being within
± 0.3 cm^3/s^2.

Using the measured static γ to determine the frequency of the plunger, we
found (to our immediate consternation) that the details of the ensuing wave propagation were utterly at variance with the resonance predictions. Either of
two conclusions may be drawn: the resonance theory is inaccurate, or the effective value of the surface tension for a surface that is continuously being deformed
is not the same as that for a static interface. Resisting (naturally) the former,
we investigated the consequences of the latter in some detail.

Considering the effective value of the surface tension coefficient, γ_e, to be
unknown, then it is a simple matter to determine this quantity by experiment.
Oscillate the plunger with a small amplitude at a frequency near that corresponding to resonance. The wavelength of the waves created can be determined then by comparing the wave signal from the probe to the driving signal,
both easily displayed on an oscilloscope as a Lissajous figure. Displacement of
the probe in the direction of propagation by an integral multiple of the wavelength
restores the same Lissajous figure (in practice, a straight line, indicating that the
wave-form at the two points is exactly in phase with the plunger motion).
The wavelength determined this way is usually precise to within one part in 10^3.
Then γ_e is determined from the dispersion relation according to $\gamma_e = (\omega^2 - gk)/k^3$.
The frequency can be measured by electronic counters to 1 part in 10^5, and the
precision of the measured γ_e is about 3 parts in 10^3, or nearly as precise as the
static tensiometer method. In all cases, the dynamically measured value was
less than the measured static value, sometimes by as much as thirty percent,
confirming our earlier suspicions. We will return to this point in the concluding
section below.

More to the point of the experiment, we can determine the actual resonant
frequency (and thence γ_e) by a simple procedure. Since $k_1 = (g/2\gamma_e)^{\frac{1}{2}}$, then in the
dispersion relation $\omega^2 = gk + \gamma_e k^3$ it is easy to see that at resonance, the first
term on the right-hand side is numerically twice the second, whatever the value
of γ_e. Then at resonance $\omega_1^2 = \frac{3}{2}gk_1$, or in terms of wavelength and period (the
directly measured variables),

$$\lambda_1 = \frac{3g}{4\pi}\tau_1^2. \qquad (4.1)$$

Figure 3 represents a 'tuning diagram,' the heavy line corresponds to (λ, τ)
satisfying the resonance conditions, which now are (4.1), or $(\lambda, \tau) = (\lambda_1, \tau_1)$
at resonance. The light lines, intersecting the tuning curves are local approximations to the dispersion curves for constant γ_e. The tuning procedure is simple:
measure a point (λ, τ) as described above, plot it on the tuning diagram, determining γ_e, then adjust the period to correspond to the intersection of that constant
γ_e curve with the resonant locus (4.1). The tuning process is in practice one of
successive convergence, usually taking no more than four steps.

As a final check on the tuning, recall that at resonance, the phase speed of the
fundamental is identical to that of the second harmonic. Accordingly, the
plunger is driven at exactly twice the (measured) resonant frequency, and the

† See *Handbook of Chemistry and Physics*, 46th ed. (1965–6).

measured wavelength is half that of the previously tuned fundamental, to within $\frac{1}{2}$%. Furthermore, besides being a necessary check on the tuning, this indicates that γ_e is identical for the two frequencies involved in the experiment, namely ω_1 and $2\omega_1$. It would be of interest to determine γ_e in the range $\omega_1 < \omega < 2\omega_1$, but this is not crucial to the proper tuning of the experiment.
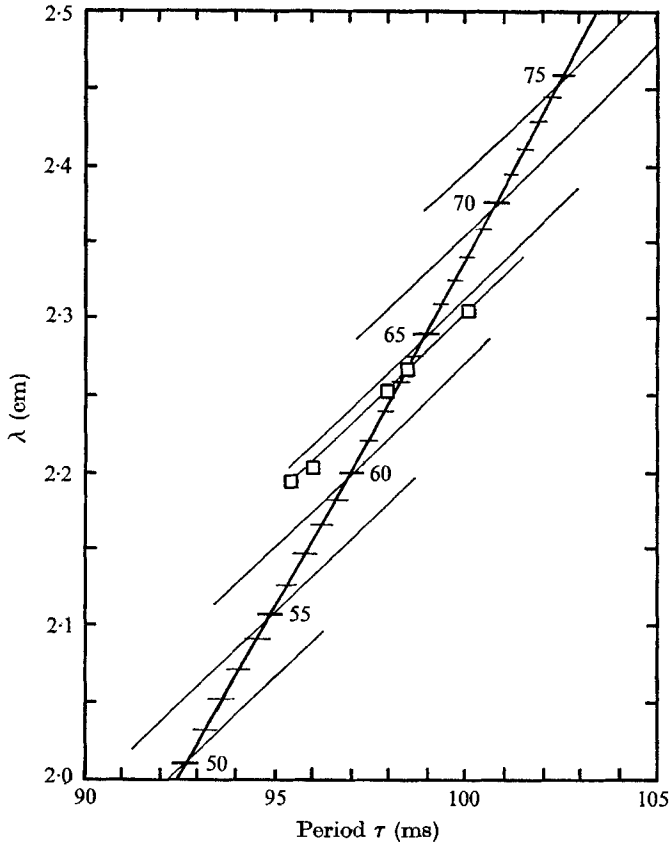

FIGURE 3. The tuning diagram. λ is the fundamental wavelength, τ the wave-maker period. The points represent the experimental determination of γ_e for the subsequent measurements.

As an experimental 'aside', we point out that a tuning diagram similar to that of figure 3 can be constructed for waves travelling at the minimum phase speed. For this case, both terms of the dispersion relation are numerically equal, and $\lambda_m = (g/\pi)\tau_m^2$. Tuning for $(\lambda, \tau) = (\lambda_m, \tau_m)$ then determines $\gamma_e(\omega_m)$. The effective surface tension measured this way always agreed with that of the first method to within the precision of the measurements. Indeed, the resonant tuning may be accomplished by determining τ_m first, then adjusting the frequency of the oscillator to $\omega_1 = (\frac{9}{32})^{\frac{1}{4}}\omega_m$. This alternative tuning procedure is less attractive experimentally than the direct tuning. It does suggest, however, that γ_e may not vary appreciably over the frequency range of interest here.

In earlier measurements on third-order gravity wave interactions, both Mc-Goldrick *et al.* and Longuet-Higgins & Smith resorted to elaborate tuning processes which involved detailed measurements of everything in sight in the neighbourhood of resonance for reasons clearly described there. In essence it was impossible to determine the 'proper tuning' in advance. In the present case, quite to the contrary, tuning is relatively easy to accomplish, obviating the necessity for detailed measurements in the neighbourhood of resonance. Indeed, to our utter delight, when carefully tuned as described above, *the interaction process is so dramatic that it can be seen by eye!* In § 5, we present the detailed histories of the interacting components and investigate the adequacy of the weak damping assumption of § 3.

5. Results of the measurements

In order to assess the adequacy of the approximations leading to the interaction equations (3.1) and figure 2, a series of experiments were performed. Before displaying the results of those measurements, it is appropriate to comment on some difficulties known to be somewhat vexatious to experimenters.

The matter of tuning the resonance, described in the preceding section is simple. That the effective, or dynamically measured, coefficient of surface tension does not agree with the accepted static values clearly indicates that the interface is not the ideal scrupulously clean one supposed in the simplest of interfacial models but in fact contaminated. We shall not be concerned with the precise chemical nature of the contamination, which presumably arises from adsorbtion of matter from the atmosphere or fall-out of minute dust and oily carbon particles, but only in its observable effects.

Given a dirty surface, then, it is clear that the dissipation of the waves will not be identical to that for a clean surface. The logarithmic decrements Δ_1 and Δ_2 of (3.1) will not be the classical expressions and must be considered unknown. In view of the form of (3.1), it is possible to determine Δ_2 directly by creating the second harmonic (a_2) alone at the plunger and measuring its decay as it progresses away from the wave-maker. Recall that, if the amplitude of the fundamental a_1 is ever zero, it remains so, and the second harmonic can propagate without interaction; i.e. the ordinate of figure 2 is a trajectory. On the other hand, it is impossible to determine Δ_1 *directly*, since the fundamental can exist only as a transient state; it must interact with its own second harmonic.

Trial measurements of Δ_2 as described above quickly revealed the not-so-surprising fact that indeed, for a dirty surface, the second harmonic was attenuated much more rapidly than for a freshly prepared relatively clean surface. Furthermore, the attenuation increased markedly, up to a point, with age of the surface, indicating that the 'dirtiness' of the surface increased with time, as we suspected.

If the characteristics of the surface are continuously changing with time, as evidenced by successive measurements of both γ_e and Δ_2, then there is no hope of obtaining detailed measurements of the interacting amplitudes, which requires some time. It would then be necessary to take elaborate precautions to keep the

surface clean, which is virtually impossible considering the physical size of the apparatus.

Fortuitously, we found that these precautions were not necessary. The continuous monitoring of the surface dirtiness revealed that usually within 3 days from filling of the tank with ordinary untreated tap water, the surface approached a kind of 'equilibrium dirtiness', after which γ_e and Δ_2 remained roughly constant for several more days. We do not wish to propose units in which dirtiness may be measured. However, a qualitative judgement may easily be made: the experiment may be performed at such time when the time constant of the dirtiness coefficients exceeds the contemplated duration of the measurements by an order of magnitude or so. As a check on the validity of this concept of 'quasi-equilibrium dirtiness,' the properties of the surface should be measured before and after the experiment. Finally, we found that the asymptotic approach to equilibrium dirtiness was repeatable, yielding (for several trails) equilibrium values for γ_e and Δ_2 differing by no more than 1 %. We feel that it is justifiable to perform the experiments on dirty water (i.e. prepared in no way).

Figure 4 represents the results of three sets of measurements shown here in the (a_1, a_2) plane. The resonance was tuned as described above, and the amplitudes of the fundamental and the second harmonic were measured as a function of distance normal to the plunger, at spatial intervals of 1 cm. The components were electronically separated with the use of an adjustable narrow-band-pass filter (Dytronics Model 720). The measured amplitudes, indicated on the figure, have been corrected for the filter shape (transfer function). The trajectories represent three series of measurements, for which the plunger was driven sinusoidally with different amplitudes, corresponding to different initial conditions.
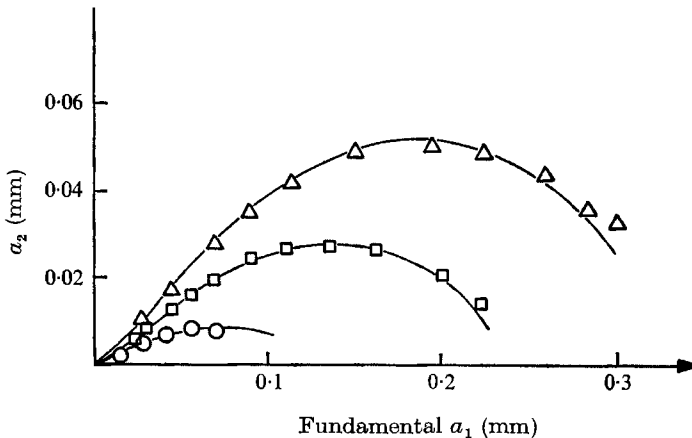

FIGURE 4. Phase plane results of three series of measurements corresponding to three different initial conditions (wave-maker amplitudes).

Now it is possible to determine the attenuation rate Δ_1 indirectly. We can consider Δ_1 to be a parameter in the interaction equations (3.1). This parameter may be varied until the solutions of (3.1) coincide with the experimental measure-

ments of figure 4. Accordingly, the equations (3.1) were set up on an analogue computer (built by us), and Δ_1 is modeled with a variable potentiometer. The analogue voltages of a_1 and a_2 are connected to the horizontal and vertical inputs of an $X-Y$ recorder (Mosley Model 7035 B). Appropriate initial conditions are set, the graph paper containing the plotted measurements placed in the machine, and the trajectories are drawn. Successive settings of the Δ_1 potentiometer eventually produce machine drawn trajectories passing through the previously plotted measured points. The accepted value of the damping coefficient then is that value for which all three trajectories best approximate the measurements.

Figure 5 presents the measurements corresponding to the outer trajectory of figure 4 as a function of distance in the direction of propagation. The upper curve is the fundamental amplitude, the lower that of the second harmonic. The line represents the computed trajectory of figure 4, or the theoretical solution.
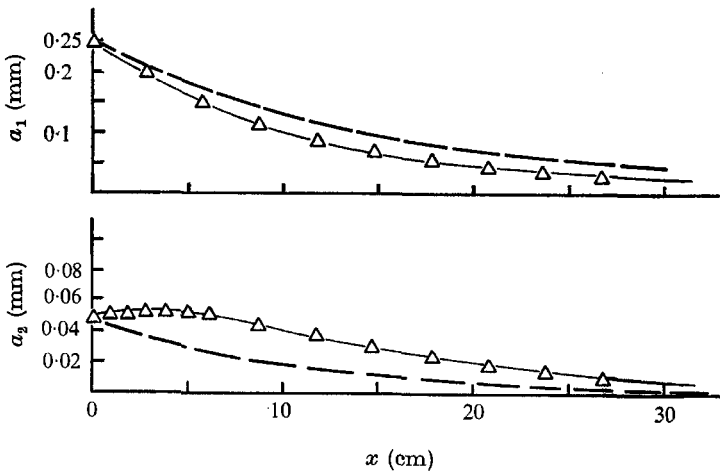
FIGURE 5. The interacting amplitudes as a function of distance compared with the theoretical result.

In order to assess the strength of the interaction with respect to the ordinary viscous attenuation, it is a simple matter to solve the dynamical equations (3.1) with the neglect of the non-linear coupling terms on the right-hand side. Each wave decays independently with logarithmic decrements Δ_i determined by the above procedure. Figure 6 summarizes the hypothetical situation. The solid lines are the measured trajectories of figure 4, the dashed lines are the trajectories computed as if there were no interaction; i.e. they represent the viscous effects alone. Again, in the lower half of figure 5, the dashed line represents the pure viscous attenuation of second harmonic a_2 that would occur if there were no interaction (and which *does* occur if it is created alone.) In the upper part of this figure, the dashed line represents the pure viscous decay of the fundamental that would occur if no interaction were taking place. The line is drawn according to the best fit Δ_1. This shows perhaps most clearly that the fundamental is a source of energy for the resonant growth of the second harmonic,

and that for some distance the resonant transfer of energy dominates the viscous decay.

The measurements presented here were all obtained within a 24 h period. Subsequently, the tank was drained and the same measurements repeated after surface equilibrium was re-established, with substantially the same results which therefore need not be repeated here. Table 1 presents a summary of the
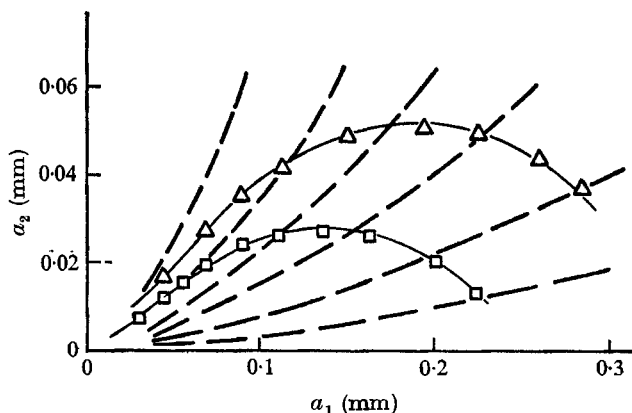

FIGURE 6. The dashed lines represent what the trajectories would be if there were no interaction, but only independent viscous decay. (Superimposed on the results of figure 4.)

surface conditions corresponding to the measurements presented and, for comparison, the same quantities for a clean surface at the same temperature, which was 20·5 °C. In the table, λ_1 and λ_2 are the wavelengths of the fundamental and the second harmonic, c the phase speed, τ_1 the period, Δ_1 and Δ_2 the logarithmic decrements. Of these quantities, the experimental value of Δ_1 is the least precise in view of the complicated manoeuvres necessary for its determination. It represents no more than the best fit by eye of the trajectories to the measured data, and no elaborate attempts have been made to determine it with the precision attained by the other figures.

		Measured (dirty surface)	Calculated (clean surface)
T (static)	dynes/cm	72·5	72·6
γ_e (dynamic)	(cm³/s²)	63·5	—
λ_1	(cm)	2·265	2·42
λ_2	(cm)	1·132	1·21
c	(cm/s)	23·01	23·79
τ_1	(ms)	98·42	101·6
Δ_1	(cm⁻¹)	0·066	0·0068
Δ_2	(cm⁻¹)	0·108	0·0194

TABLE 1. Summary of the measurements.

Finally, there is the question of relative phase which determines the wave form. According to the analysis, the phase difference between the two interacting components is $\frac{1}{2}\pi$. Figure 7 (plate 1) is a photograph of two oscilloscope traces showing the wave form. The vertical input is the wave form directly from the output of the wave-probe device, the vertical sensitivity on both photographs is 0·02 mm (wave elevation) per large division, and the horizontal sweep rate is 20 ms/div. For the upper photograph, the probe is about 11 cm from the plunger face and for the lower, about 25 cm farther downstream. In both cases, the relative phase is closely $\frac{1}{2}\pi$, and in all cases during the course of this investigation, this phase difference remained constant with propagation distance. Apparently, the viscous attenuation (for this case) does not affect the relative phase between the interacting components. Further, for this case of resonance, the actual wave form bears no similarity with the symmetrical, but steady state profiles given by Wilton (1915) and others subsequently.

6. Further comments and summary

It is appropriate here to include some further thoughts on the nature and effects of the surface contamination. Miles (1967) confronted the problem of surface wave damping due to viscous dissipation at and in the neighbourhood of a free surface covered by a viscoelastic surface film from an analytical point of view, attempting with some success to explain earlier experimental observations. In particular, among those controlled (from the chemical point of view) experiments, Davies & Vose (1965) measured the damping of capillary ($\lambda < 0.5$ cm) waves on both clean and meticulously prepared contaminated surfaces. Among their objectives was the answer to the following question: 'Does the Kelvin equation (alternatively, our dispersion relation (2.2)) give the equilibrium surface tension of film-covered surfaces (i.e. when the surface tension fluctuates between the crests and troughs)?'

In general, the damping at a clean surface results from viscous energy dissipation in the bulk of the fluid. The surface is completely mobile and the logarithmic decrement is well known as $\Delta = 2\nu k^2/U$. On the other hand, if a surface layer is present, the surface tends to contract at a crest and expand at a trough so that surface tension stress gradients are produced by differential surface concentrations of the contaminant, the effect being an increased rate of energy dissipation. For a surface immoblized by a surface film (i.e. which has no horizontal velocity components), Lamb (1932) obtained for the damping

$$\Delta_{imm} = (\nu\omega k^2/8U)^{\frac{1}{2}},$$

which is greater than that for a clean surface for all but the shortest of capillary wavelengths.

Davies & Vose further point out that, if the surface dilitational viscosity is negligible with respect to the surface compressional modulus, then for values of this modulus intermediate to the fully mobile and completely immobile surfaces the damping can be approximately twice as great as Δ_{imm}. Miles (1967, figure 1) determines a measure of the damping that owes its existence to the

presence of a surface film and presents this measure graphically as a function of the surface compressional modulus for several values of the dilitational viscosity, clearly delineating the conditions for which the damping is greater than Δ_{imm}.

From our experiments (see table 1) the measured decrements are $\Delta_1 = 1\cdot6\,\Delta_{1\,imm}$ and $\Delta_2 = 1\cdot3\,\Delta_{2\,imm}$, the latter being more precise for reasons mentioned above. The measured decay agrees with the immobile calculations much more closely than with the clean surface calculations which suggest a conjecture: perhaps the 'approach to equilibrium dirtiness' described in § 5 is, in view of the continuous adsorption or deposition at the surface, in reality an 'approach to surface immobility'. This conjecture is, of course, impossible to establish firmly on the basis of our experiments, since the precise composition of the film is unknown, but suggests further investigation along these lines under carefully controlled conditions.

Davies & Vose, in addressing themselves to the posed question on the applicability of Kelvin's formula, concluded that it was accurate to within $1\cdot5\%$ on clean water, and further, is approximately valid for film covered surfaces, even though γ now varies between the crests and troughs. We disagree with their second conclusion. It is clear from our results that at the time of the experiments, the measured equilibrium surface tension was $72\cdot5$ dynes/cm, whereas the value determined under dynamical conditions from Kelvin's formula was $63\cdot5$ dynes/cm, or approximately $12\cdot5\%$ smaller. The Kelvin formula in our case does *not* give the equilibrium surface tension, but apparently an effective average over a wavelength. But then, in our dynamical problem, there is no compelling reason why the equilibrium value should be relevant. What the Kelvin formula does give for contaminated surfaces is the correct value for the 'dynamic' surface tension, as evidenced by the success of the tuning in a clear cut resonant dynamical problem.
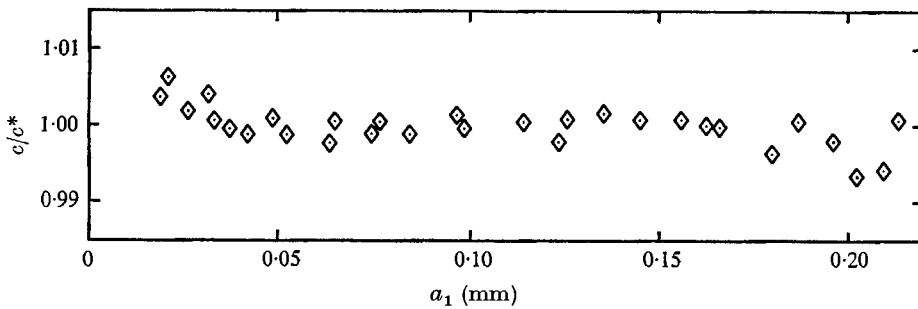
FIGURE 8. Phase speed as a function of wave amplitude at resonance. From table 1, $c^* = 23\cdot01$ cm/s.

It is natural to ask at this point whether the effective surface tension varies with the rate of straining of the surface film at constant frequency, which is proportional to the amplitude of the waves. Accordingly, the phase speed at resonance was measured for a range of amplitudes intermediate to those obtaining in the experiments. The results are shown in figure 8. The ratio of measured phase

speed c to that determined by the value of γ_e from table 1 ($c^* = (\frac{9}{2}\gamma_e g)^{\frac{1}{4}}$) is shown as a function of the measured amplitude of the wave. The variation in the speed is less than 1 %, which is close to the overall precision of the measurements and we may conclude that the effective surface tension remains close to its determined value, at least over much of the range of the experiment.

As mentioned before, due to the sharpness with which the resonance can be tuned, it is not necessary to make detailed measurements in the neighbourhood of the resonant frequency such as were necessary for our earlier gravity wave interaction studies. It is worthwhile to present some information off tune in view of the conclusion that will ultimately be drawn. Figure 9 (plate 2) presents photographs from the oscilloscope of the wave forms corresponding to (a) frequency 13 % lower than resonant (8·82 c/s) and (b) 11 % higher than resonant (11·7 c/s). For both pictures, each vertical major division represents 0·02 mm wave height and the horizontal sweep is 20 ms/div. The upper (9a) is a Stokes, or gravity-type profile while the lower (9b) is a Crapper or capillary-type profile, for which the crests are flattened and the troughs sharpened. Both profiles are in qualitative agreement with the (non-singular) results of Wilton (1915). The phase of the second harmonic constituent relative to the fundamental, zero for the upper and π for the lower, remains constant as the wave progresses the tank, and the second harmonic component never grows. That is, in both cases, the wave form becomes closely simple harmonic as the wave attenuates with distance from the plunger. Sufficiently far from a resonance, then, the Stokesian analysis certainly should be a good approximation.

Finally, then, the conclusion that must be drawn from these experiments is inescapable. The influence of viscous dissipation suggested earlier seems to be entirely adequate to the order considered here. But, more important, we have demonstrated (again) that under resonant conditions and with the initial conditions as chosen here, there cannot be a uniform wave profile.

REFERENCES

BARAKAT, R. & HOUSTON, A. 1968 Non-linear periodic capillary-gravity waves on a fluid of finite depth. *J. geophys. Res.* **73**, 6545–6555.

BENJAMIN, T. B. & FEIR, J. E. 1967 The disintegration of wave trains on deep water. *J. Fluid Mech.* **27**, 417–430.

BENNEY, D. J. 1962 Non-linear gravity wave interactions. *J. Fluid Mech.* **14**, 577–584.

CRAPPER, G. D. 1957 An exact solution for progressive capillary waves of arbitrary amplitude. *J. Fluid Mech.* **2**, 532–540.

DAVIES, J. T. & VOSE, R. W. 1965 On the damping of capillary waves by surface films. *Proc. Roy. Soc. Lond.* A **286**, 218–234.

HARRISON, W. J. 1909 The influence of viscosity and capillarity on waves of finite amplitude. *Proc. Lond. Math. Soc.* (2), **7**, 107–121.

KAMESVARA RAV, J. C. 1920 On ripples of finite amplitude. *Proc. Indian Ass. Cultiv. Sci.* **6**, 175–193.

LAMB, H. 1932 *Hydrodynamics.* Cambridge University Press.

LONGUET-HIGGINS, M. S. 1962 Resonant interactions between two trains of gravity waves. *J. Fluid Mech.* **12**, 321–332.

LONGUET-HIGGINS, M. S. & SMITH, N. D. 1966 An experiment on third-order resonant wave interactions. *J. Fluid Mech.* **25**, 417–436.

McGOLDRICK, L. F. 1965 Resonant interactions among capillary-gravity waves. *J. Fluid Mech.* **21**, 305–331.

McGOLDRICK, L. F., PHILLIPS, O. M., HUANG, N. E. & HODGSON, T. H. 1966 Measurements of third-order resonant wave interactions. *J. Fluid Mech.* **25**, 437–456.

MILES, J. W. 1967 Surface-wave damping in closed basins. *Proc. Roy. Soc. Lond.* A **297**, 459–475.

PHILLIPS, O. M. 1960 On the dynamics of unsteady gravity waves of finite amplitude. Part 1. The elementary interactions. *J. Fluid Mech.* **9**, 193–217.

PHILLIPS, O. M. 1967 Theoretical and experimental studies of gravity wave interactions. *Proc. Roy. Soc. Lond.* A **299**, 104–119.

PIERSON, W. J. & FIFE, P. 1961 Some non-linear properties of long crested periodic waves with lengths near 2·44 cm. *J. geophys. Res.* **66** (1), 163–179.

RAYLEIGH, LORD 1917 On periodic irrotational waves at the surface of deep water. *Phil. Mag.* **33**, 381–389.

SIMMONS, W. F. 1967 A variational method for weak resonant wave interactions. From Ph.D. Thesis, Department of Mechanics, The Johns Hopkins University. See also *Proc. Roy. Soc. Lond.* A **309**, 551–575 (1969).

STOKES, G. G. 1847 On the theory of oscillatory waves. *Trans. Camb. Phil. Soc.* **8**, 441–455.

SULLIVAN, J. B. 1966 Steady state interactions among intersecting trains of capillary-gravity waves. *Geophysical Sciences Laboratory Report* no. TR66-7, New York University.

WILTON, J. R. 1915 On ripples. *Phil. Mag.* (6) **29**, 173.
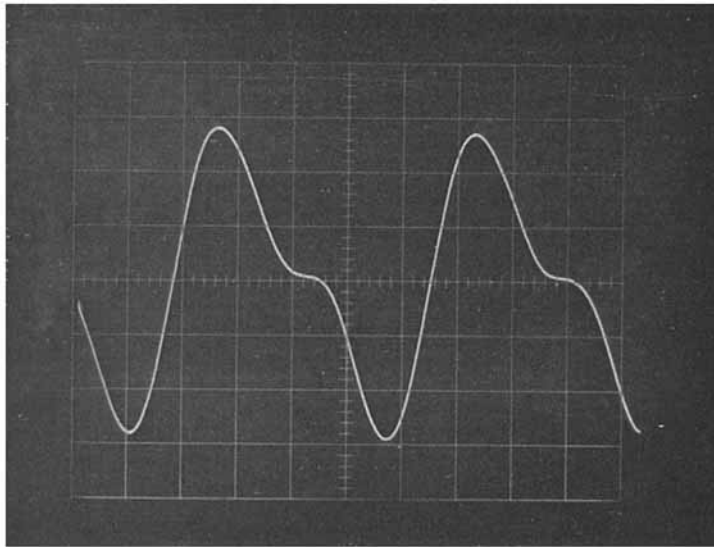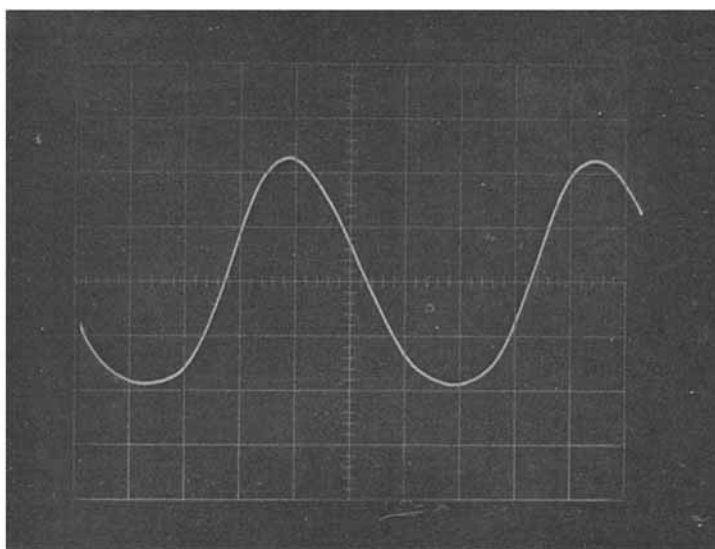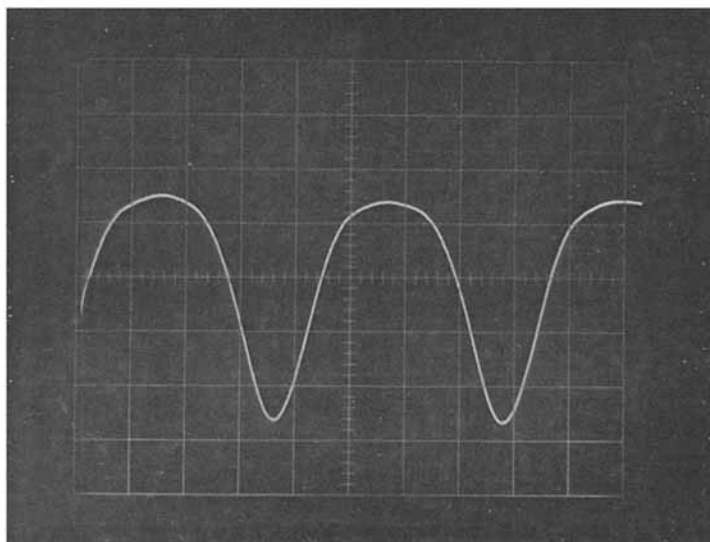
(a)
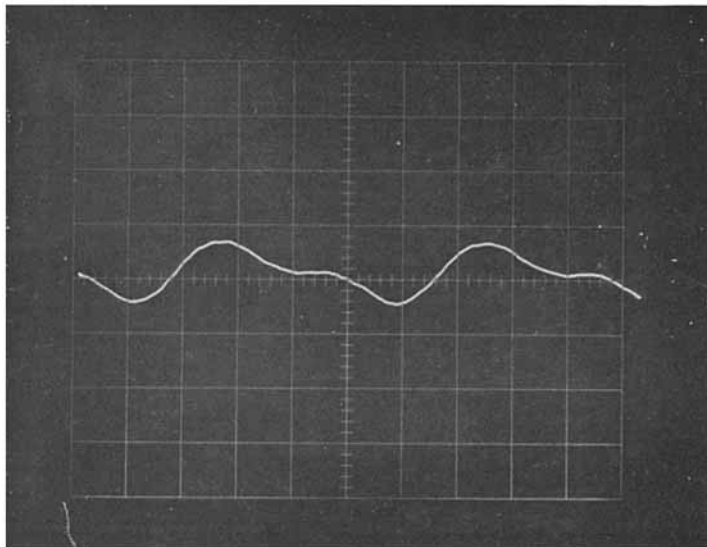
(b)

FIGURE 7. (a) Oscilloscope trace showing the phase difference, at 11 cm from the wave-maker. Total wave amplitude is about 0·11 mm. (b) Same conditions as (a) but 25 cm farther from the wave-maker.

(a)

(b)

FIGURE 9. Wave forms off resonance. (a) Frequency 8·82 c/s. Gravity type. (b) Frequency 11·0 c/s. Capillary type.

McGOLDRICK